



Many-body study of the photoisomerization of the minimal model of the retinal protonated Schiff base

Adriano Mosca Conte^{a,*}, Leonardo Guidoni^b, Rodolfo Del Sole^{a,1}, Olivia Pulci^{a,1}

^a MIFP, NAST, ETSF, CNR INFM-SMC, Università di Roma Tor Vergata, Via della Ricerca Scientifica 1, Roma, Italy

^b Università degli Studi di L'Aquila, Dipartimento di Chimica e Materiali, Via Campo di Pile, 67100, L'Aquila, Italy

ARTICLE INFO

Article history:

Received 25 June 2011

In final form 16 September 2011

Available online 21 September 2011

ABSTRACT

We investigate the optical properties of the *tZt-penta-3,5-dieniminium* cation, a simplified model for the protonated Schiff base of 11-*cis* retinal in rhodopsin, along the isomerization pathway by ab-initio calculations based on Many-Body Perturbation Theory using the GW method and the Bethe–Salpeter equation. Our calculations are carried out on a few significant CASSCF geometrical configurations of the isomerization minimal energy path taken from the literature. Our excitation energies are qualitatively in agreement with previous Quantum Monte Carlo and post-Hartree–Fock calculations. We also employ TDDFT based methods, and investigate the outcome of using different approximations and several exchange–correlation functionals.

© 2011 Elsevier B.V. All rights reserved.

1. Introduction

The mechanism of vision is present in most living creatures [13,15,28]. In animals this mechanism is supported by a complex apparatus, but the ability to transform external optical perturbations in chemical signals is also present in the most primitive forms of life such as bacteria [27]. In all cases the first and most important step of the mechanism is the photoisomerization of the rhodopsin chromophore: the protonated Schiff base of 11-*cis* retinal. In animals the chromophore, formed by a polyenic chain terminating by a β -ionone ring, is covalently bonded to the residue Lys 296 of rhodopsin. Upon the absorption of a photon, its geometrical conformation changes from 11-*cis* to all-*trans* by a rotation along the axis connecting two carbon atoms of the polyenic chain (C_{11} and C_{12} , see Figure 1). Despite the importance of this process and several experimental [16,17,20,26,33] and theoretical studies [5,6,9,11,25,37–39,45–49] on this topic, the photoisomerization mechanism is not yet fully understood [19,29].

A theoretical description and evaluation of the efficiency and velocity of the photoisomerization of the protonated Schiff base of 11-*cis* retinal is possible only by a very precise calculation of the excited-state energies along all the phases of the isomerization. This issue, together with the size of the system, represents a great challenge for the most accurate chemical and physical theoretical techniques that compute optical properties in molecules and

solids. For this reason, as a first step, many theoretical methods have been tested on a simpler smaller-size molecule, the *tZt-penta-3,5-dieniminium* ($C_5H_6NH_2^+$), that is a Minimal Model (MM) of the retinal protonated Schiff base [12,43,32,8,18]. This 14-atom compound is a short conjugated chain (see Figure 1) sharing many features with the protonated Schiff base of the retinal [12]. Actually, the photoisomerization path of the Schiff bases appears to be quite sensitive to the length of the conjugated chain model. Hence it may be only roughly representative of the actual rhodopsin retinal. Nevertheless, despite the simplicity of the MM, the accuracy required for the study of its photoisomerization stretches the predictive power of most theoretical spectroscopy methods to their limits.

In this work we study the photoisomerization of the MM within Many-Body Perturbation Theory (MBPT) [10] using the GW approach [14] and the Bethe–Salpeter equation [36]. Very recently, this method has been successfully applied to the calculation of vertical excitations of biological chromophores and photoactive molecules [21–23]. Here, we investigate the reliability of MBPT to describe the excited state energy surfaces along the photoisomerization pathway. Atomic coordinates, taken from supporting material in Ref. [12], were calculated within CASSCF. More refined geometries, obtained within CASPT2 [18,32], and within Coupled Cluster (CC2) [43] have recently challenged the CASSCF minimal energy path. CC2 calculations [43] of potential energy surfaces of several Schiff bases have been compared to those obtained using TDDFT methods. While in many cases the two approaches give the same qualitative results, significant differences are found for some single-bond torsions in longer protonated Schiff bases. Similar calculations have been done using CASPT2 [8,18,32] for several photoactive molecules. Differences of the order of 0.01–0.02 Å

* Corresponding author. Fax: +39 06 202 3507.

E-mail addresses: adrianomoscaconte@gmail.com (A.M. Conte), leonardo.guidoni@univaq.it (L. Guidoni), rodolfo.delsola@roma2.infn.it (R. Del Sole), olivia.pulci@roma2.infn.it (O. Pulci).

¹ Fax: +39 06 202 3507.

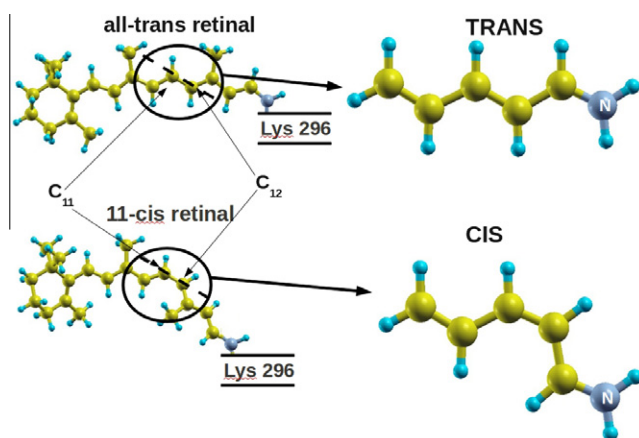


Figure 1. Protonated Schiff base of the retinal (on the left) and protonated Schiff base minimal model (on the right) in *cis* and *trans* configurations. Dashed lines indicate the rotation axis during the isomerization process.

have been observed comparing CASPT2 and CASSCF excited state geometries. Concerning the MM isomerization path, the full-CASPT2 calculation give a very small barrier in the S_1 energy path between the *cis* and the *CI* configuration, whose energy is in any case smaller than the *cis* energy and should not in principle induce an increase of the isomerization time. CASPT2 calculations performed on CASSCF geometries give no barriers at all. As a consequence, MBPT calculations performed on geometry paths calculated with different methods could give qualitatively different results. This is why it is important to compare the results of the different methods by using the same geometries.

Our MBPT-based calculations results depend on the reliability of the underlying CASSCF geometries, and in principle they can not clarify the details of the true photoisomerization path of the MM. The goal of the present work is, indeed, to explore the reliability of MBPT to describe the excitation energies along the proposed path, and compare our results with those obtained by TDDFT and CASPT2 [8] performed using the very same CASSCF trajectory.

We found qualitative agreement with previous Quantum Monte Carlo [41] and CASPT2 calculations [8]. We also performed Time Dependent Density Functional Theory calculations on the same CASSCF-optimized geometries, and found some small differences in the energy path.

We investigate the origin of these discrepancies by analyzing the effect of several possible approximations to the TDDFT exchange–correlation kernel.

The Letter is organized as follows: in the next section we present state-of-the-art calculations of the photoisomerization of the MM, and discuss open issues. In Section 3, we revise the main theoretical tools used in our investigation (GW, BSE and TDDFT), and very briefly discuss the methods used in previous works. In Section 4 section we present and discuss our results, and compare them to results of other theoretical methods. The main achievements of our research are summarized in Section 4.

2. Minimal Model of the retinal: open problems

Like in the case of the retinal, the most debated topic concerning the MM is the qualitative description of its photoisomerization pathway. The scientific community is divided between two possible scenarios [19] (see Figure 2): a two-state model, involving the ground state S_0 of the MM and its first excited singlet state S_1 , and a three-state model, involving a further excited singlet state S_2 . According to the first model (upper left panel, Figure 2), the ground state of the Schiff base has two minima corresponding to *cis* and *trans* conformations. A rotation of the molecule around the axis connecting

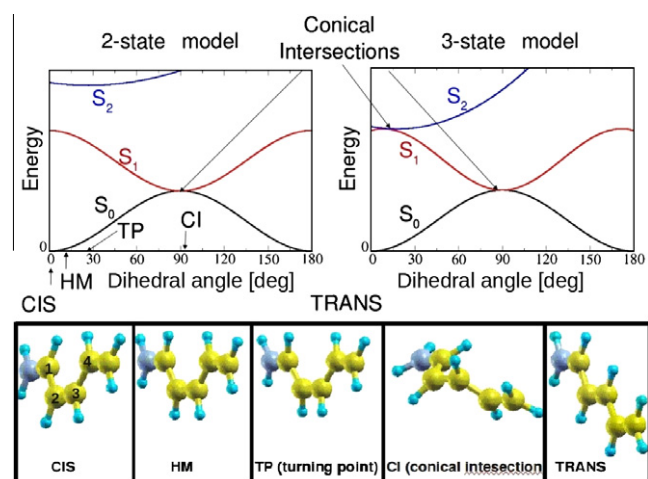


Figure 2. Qualitative description of the two-state model (upper-left panel) and three-state model (upper-right panel). Lower panel: main geometry configurations of the protonated Schiff base minimal model during its isomerization. The dihedral angle is the one involving atoms 1, 2, 3 and 4.

the two internal carbon atoms breaks the double bond between the two carbon atoms, and induces an increase of the total energy that reaches its maximum after a rotation of about 90° . *Cis* and *trans* ground state energies are therefore separated by a barrier of about 2 eV. On the contrary, the first excited singlet state S_1 has an energy of about 4 eV [12] above the ground state in *cis* and *trans* configurations, and decreases in rotated geometrical conformations. The minimal energy corresponds to a rotation of about 90° at which a conical intersection between the S_0 and S_1 surfaces occurs.

In the second model (right upper panel, Figure 2), the S_2 state forms a second conical intersection with the S_1 state inducing a small energy barrier in the S_1 state along the path connecting the *cis* conformation to the S_0 – S_1 conical intersection. This can be of great importance for the determination of the efficiency and the velocity of the isomerization. It is estimated that, due to this small energy barrier, the reaction time of the three-state process could be one order of magnitude longer than a two-state one [20]. The choice of the best model concerns both the retinal and the MM, and does not present an easy solution in both cases. Therefore, besides the interesting properties of the system itself, the MM is an ideal candidate to test theoretical methods and understand their limits in predicting the properties of photoactive molecules. In previous theoretical works [21,23] optical properties of several photoactive molecules have been calculated using MBPT for fixed geometries. Here we also study the excited-state energy surfaces of the MM in some of the geometries of the isomerization path. Hence, a goal of this paper is also to assess the validity of MBPT methods to reproduce results obtained within other high level quantum chemical tools.

Despite the small size of the MM, the qualitative description of its photoisomerization is anything but easy to simulate. A clear clue of the present difficulties is that different methods give different results. Some efforts to predict the photoisomerization trajectory using TDDFT failed because of the inability of most of the approximations for the exchange–correlation kernel to correctly compute the excited-state forces of Schiff bases [50].

Following the determination of the trajectory, the second problem to solve is the calculation of the excited state energies. Once again, different methods give different results, even when the same coordinates are used [8]. This is evident by comparing post-Hartree–Fock based CASPT2 [12,8], DMC [41], and TDDFT excited state energies [50]. In Ref. [8], CASPT2 calculations performed on a CASSCF-trajectory find a very small barrier (< 0.1 eV) along the isomerization pathway. Apparently, no energy barrier is found within

diffusion Monte Carlo calculations performed on Restricted Open Shell Kohn–Sham (ROKS) minimal energy path (MEP) [41] although this observation should be verified by a calculation of the S_1 energies on a more dense sampling. A higher barrier was found when using TDDFT both on CASSCF[8] and on ROKS [41] coordinates. Therefore TDDFT calculations still support the two-state model. The difference with the CASPT2 results is that the S_1 energy of the geometrical configuration corresponding to the top of the energy barrier has a higher energy than the S_1 *cis* energy. This could strongly affect the excited state dynamics of the system. Given the importance of the geometry on the optical properties of the MM, the different choice of coordinates introduces a further complication for the task of comparing the results between the various methods and interpreting their dissimilarities. The few available experimental data cannot provide any help [2,3,7]: to the best of our knowledge, experimental optical spectra are at present available only for molecules with a similar structure (but not exactly the same) and not for molecules in gas phase, but only in solution or in solid-state phase. Moreover, experimental information is not available for the intermediate configurations, but only for the *cis* one.

The discrepancies between TDDFT calculations and CASPT2 are generally attributed to the inability of most of the approximations used in TDDFT to correctly describe the electron-hole interaction in charge-transfer materials. This interaction is better treated by quantum many-body techniques such as the GW method [10] combined with the Bethe–Salpeter equation (BSE) [36]. The typical dimension of the matrices involved in the BSE approach is given by the product of the number of occupied and unoccupied states ($N_o \cdot N_u$). From the point of view of the computational resources, this represents an advantage with respect to post Hartree–Fock methods whose matrices are typically significantly larger depending on the number of double, triple, ...n-ple, excitations involved. The purpose of the present work is to calculate the optical absorption spectra and ground and excited states energies of the MM by GW and BSE and to assess the validity of these methods on representative geometrical configurations along the photoisomerization pathway.

3. Methods

3.1. General overview

The calculation of optical properties in many systems requires the use of very high level techniques as well as large computational resources. The methods for their prediction can be collected in different categories such as post Hartree–Fock, Monte-Carlo, many-body perturbative techniques [14] and TDDFT [40]. In this work, for the calculation of the optical absorption spectrum and excited state energies we used methods belonging to the last two categories: the TDDFT Casida algorithm [4], and a combination of two different quantum many body techniques (the GW method [10] for the calculation of the electronic levels, and the Bethe–Salpeter equation [36] for the evaluation of the optical spectrum). The main difference between TDDFT and MBPT is the mathematical function characterizing the state of the system. In TDDFT the main role is played by the charge density, while in many-body perturbative methods the main character is, instead, the Green function. These two approaches also differ in the way of facing the problem of finding an expression for the electron–electron interaction that is included in the equation giving the optical spectrum. The many-body perturbative methods firstly proceed by solving the equations for a non interacting system (usually with the help of a mean field theory), and then by treating the electron–electron interaction as a perturbation of the system, giving an approximate solution of an

exact eigen-problem. The methods based on TDDFT give instead an exact solution to an approximated Hamiltonian whose components are functionals of the density. Both approaches are widely discussed in the literature [14,10,31,36,40,4].

The excitation energies ϵ_n^{exc} obtained by the two approaches have been used to calculate the excited state energies E_n by the addition of the ground state energy E_{GS} obtained by DFT:

$$E_n = E_{GS}(DFT) + \epsilon_n^{exc} \quad (1)$$

In this work we compared our results with the ones obtained by CASPT2 [8]. The second-order perturbation corrections to this post Hartree–Fock method are commonly applied to obtain accurate excited state energies.

An alternative method is to calculate the excited eigenstates of the system by using Variational Monte-Carlo (VMC) and Diffusion Monte Carlo (DMC) techniques [41], which are also very accurate ab-initio methods. We compare our results obtained with both methods.

3.2. Computational details

We calculated the ground-state energy of the MM in the most representative geometrical configurations of the photoisomerization pathway: *cis*, *HM*, *TP* (turning point), *CI* (conical intersection) and *trans*. All these configurations are accurately described in Ref. [12] and correspond respectively to a rotation around the main molecular axis of about 0°, 12°, 25°, 90°, and 180° (see Figure 2). Since the geometries of the MEP do not correspond to a rigid rotation of the MM, but also involve a stretching of the bonds, especially in the first steps, the MEP in Figures 4 and 5 is reported in atomic units that corresponds to the sum of the absolute value of all atomic coordinate displacements, rather than by simply reporting the dihedral angle. Atomic coordinates were taken from Ref. [12] and lay on the minimal energy path of the S_1 state. We then applied TDDFT and GW plus BSE to these configurations to determine their optical spectrum. We used a cutoff of 40 Ry for DFT wavefunctions (corresponding to 35053 plane waves), an FCC periodic cell with a lattice constant of 32 a.u., and norm-conserving pseudopotentials generated by using a BLYP functional (Von Barth–Car parametrization for H atom and Trouiller–Martins for the other types of atom). We used 12051 plane waves and 1000 Kohn–Sham electronic energy levels to calculate the screened potential W . This same amount of plane waves and 200 energy levels were used to solve the BSE. The interaction with periodic images was eliminated by using the Tuckerman–Martyna [24] method in DFT calculations, and by a cutoff in real space on the Coulomb potential in the GW and Bethe–Salpeter calculations, as in Ref. [30]. All these parameters were chosen after accurate convergence tests.

DFT calculations have been performed using the QUANTUM ESPRESSO plane waves code www.quantum-espresso.org. To solve the BSE we used the EXC code (www.bethe-salpeter.org). TDDFT calculations with BLYP functional have been performed using the CPMD code (www.cpmid.org), whereas for TDDFT-B3LYP calculations we have used GAUSSIAN (www.gaussian.org) with a 6-31+G* basis set.

4. Results and discussion

4.1. 2-state versus 3-state model

In Figure 3 we report the BSE spectrum in the *cis* geometry. The two lowest energy peaks were found at 3.75 eV and 5.40 eV corresponding to the S_0 – S_1 and S_0 – S_2 optical transitions, in good agreement with CASPT2 calculations of Refs. [12,8] (respectively 4.0 eV [12,8] and 5.35 eV [12]). As shown in Figure 3, the first peak under-

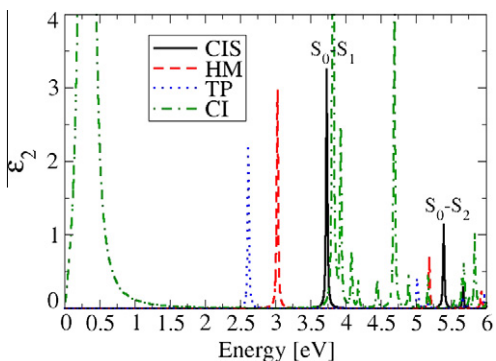


Figure 3. BSE absorption spectrum of the MM in *cis*, *HM*, *TP*, and *CI* geometries. A Lorentzian broadening of 0.01 eV has been used.

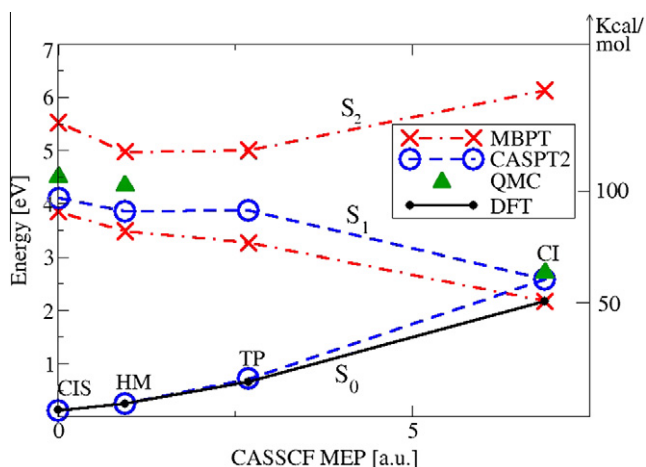


Figure 4. Ground and excited state levels along the CASSCF minimal energy path (MEP, described in the text) calculated by DFT (S_0), and by GW and BSE (S_1 and S_2). Different colors indicate different methods: black for DFT, red for MBPT, blue for CASPT2[8], and green triangles for DMC[41]. (For interpretation of the references to colour in this figure legend, the reader is referred to the web version of this article.)

goes a red shift in the first phases of the isomerization going from *cis* to *CI* through *HM* and *TP*.

For each configuration, the energies of the S_1 and S_2 states were obtained by adding the optical transition energies S_0-S_1 and S_0-S_2 , calculated with the inclusion of quasiparticle and excitonic effects to the ground-state energy, following Eq. 1. The S_1 energy decreases in passing from the *cis* to the *CI* geometry (see Figure 4). We can observe that S_1 and S_2 states are separated in energy by more than 1 eV, and that the S_1 energy has a negative trend in passing from *cis* to *HM* and then to *TP* configuration. This suggests that S_1 and S_2 states do not form conical intersections like in the two-state model interpretation of the MM isomerization pathway (in agreement with CASPT2[12,8] results). In carrying out our MBPT calculations we have found that special care had to be paid in the construction of the excitonic Hamiltonian. In fact, it turned out to be important to include in the excitonic Hamiltonian also the coupling part (see Ref. [36]) in our calculations. Refs. [21,23] put in evidence the importance of coupling for an accurate quantitative description of photoactive-molecule optical properties. Here the role of the coupling is even more relevant, giving a different qualitative description of the S_1 energy surface. Actually, a simpler solution of the BSE, in the commonly used resonant approximation, produces a different qualitative description of the isomerization (see Figure 5). In this approximation, the energies predicted for the *cis* configuration are similar to the ones predicted by using the full excitonic Hamiltonian. Nevertheless, the S_1 state presents

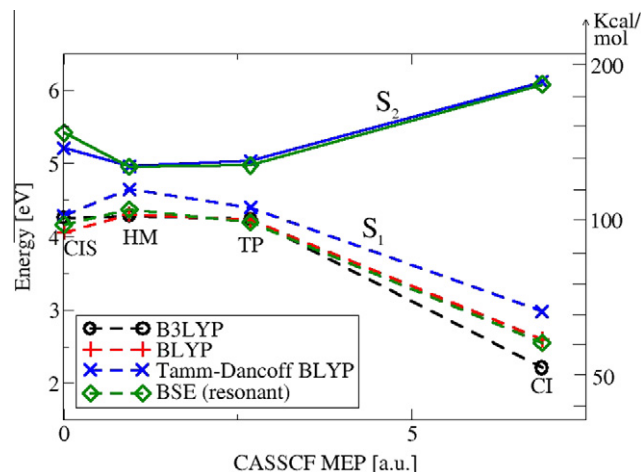


Figure 5. S_1 and S_2 excited state levels along the CASSCF minimal energy path (MEP, described in the text) calculated with TDDFT (with and without the Tamm-Dancoff approximation) and within GW + BSE (in the resonant approximation).

a barrier of 0.2 eV and its energy near the *HM* configuration is slightly closer to the S_2 state energy than in the BSE-coupling case. These features are more in agreement with the 3-state model than with the 2-state one. Hence, the coupling part of the excitonic Hamiltonian cannot be neglected.

4.2. TDDFT results

We applied TDDFT to the MM by using the same atomic CASSCF coordinates. We initially used a BLYP functional and the Tamm-Dancoff approximation. Figure 5 indicates that in the region between *cis* and *HM* configurations along the MEP, there is a positive energy trend of the S_1 state and S_1 and S_2 energies are very close to each other. Given the similarity between the Tamm-Dancoff approximation in the TDDFT and the resonant approximation in the BSE, and given the fact that in BSE the introduction of the coupling in the excitonic Hamiltonian is determinant for the evaluation of the S_1 energy along the minimal energy path, we went beyond the Tamm-Dancoff approximation. As a result, the barrier was reduced, but did not disappear. This has been checked also using different functionals (BLYP, LDA or PBE [35,34]). A more sensitive reduction of the *HM-cis* energy difference and the opening of the S_1-S_2 energy gap was observed by using the hybrid B3LYP functional. Our results are very close to those of Ref. [8]. In contrast to the other functionals, in B3LYP the exchange part of the kernel is partially nonlocal and its long-range part is better described. The correlation is instead treated by a local BLYP functional. An interesting point would be to perform these calculations by using a TDDFT kernel obtained using many-body techniques [44,1]. This would enable to consider also the non-locality of the correlation part of the kernel. The importance of this last point is stressed also by the fact that the results obtained by using methods such as CASPT2, DMC, GW + BSE, that consider the non-locality of the exchange-correlation energy, do not have points along the minimal energy path of the S_1 state where the S_1 energy is higher than in *cis*.

4.3. Charge transfer analysis

Charge transfer, induced inside a molecule by the interaction with external electromagnetic fields, is usually not well described within the usual TDDFT approximations. This is a consequence of the crucial role played by the long-range part of the exchange-correlation kernel in these cases. This gives a further reason to inspect the charge distribution changes during the isomerization. In *cis* geometry, the TDDFT electronic transitions involved in the first

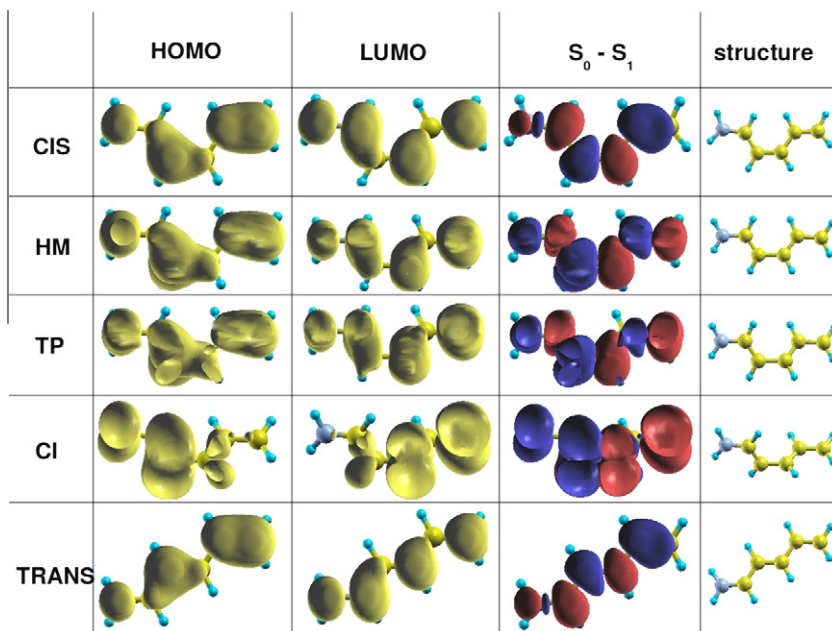


Figure 6. DFT charge distribution function of HOMO and LUMO, and charge transfer characterizing the S_0 – S_1 transition for all the geometry configurations (blue positive charge, red negative charge). (For interpretation of the references to colour in this figure legend, the reader is referred to the web version of this article.)

peak are HOMO–LUMO (74%), HOMO–(LUMO + 1) and (HOMO-1)–LUMO, and for the second peak 100% (HOMO-2)–LUMO. The HOMO charge distribution, displayed in Figure 6, is typical of π bonds between the carbon atoms. The HOMO state gives therefore a fundamental contribution to the rigidity of the molecule. On the contrary, the LUMO charge distribution does not lie on the double bonds of the polyenic chain. Both the first and the second transitions have a $\pi - \pi^*$ character. In this geometry therefore the interaction with the light weakens the double bonds but does not induce a considerable charge transfer along the chain. A similar behavior is observed in *HM* and *TP* configurations. The situation is different when the MM starts to rotate. When the dihedral angle reaches 90° (*CI* geometry) the HOMO charge distribution (shown in Figure 6) is mainly concentrated around the N atom. The first peak is 100% HOMO–LUMO transition, and it involves a substantial charge transfer from the N-side of the molecule to the opposite side. The charge distributions of S_0 and S_1 states calculated by TDDFT agree qualitatively with those calculated by CASPT2 [8]. Therefore the fact that the trend of the S_1 energy along the isomerization pathway calculated by TDDFT is different from the one calculated by other methods is apparently not a consequence of a sensitive difference of the charge distribution. The discrepancies in the S_1 energy in *HM* and *TP* configurations are very small, but sufficiently large to give a different qualitative description of the isomerization process. Since three accurate theoretical methods (GW + BSE, CASPT2 and DMC) give the same qualitative results, the different trend of the S_1 energy in the first steps of the isomerization pathway is probably to be attributed to the insufficient accuracy of the most commonly used approximations to evaluate the TDDFT exchange–correlation kernel.

5. Conclusions

We studied the Minimal Model (MM) of the retinal protonated Schiff base isomerization process using the many body Perturbation Theory, in particular the GW + BSE method. The calculations of optical properties were carried out on a few significant geometrical configurations along the isomerization pathway whose coordinates were calculated in a previous work [12] by the CASSCF

method. The S_1 energy decreases in passing from *cis* to *HM* and *TP* geometries. In all the configurations calculated, the S_1 – S_2 energy gap is larger than 1 eV. These results, although taken on a few representative points on a CASSCF MEP [12], may suggest the validity of the two-state model. A further investigation including gradients in the MBPT methods for the calculation of excited-state forces and the consequent evaluation of the MEP would be extremely useful to confirm this picture. It is worth noticing that qualitatively different results are obtained if the coupling between the resonant and antiresonant part of the excitonic Hamiltonian is neglected. In systems studied in Refs. [21,23], the discrepancies induced by neglecting the coupling had a quantitative character only. TDDFT calculations have been performed with several functionals and with and without the Tamm–Dancoff approximation. A positive trend of the S_1 energy is predicted along the S_1 MEP in the region between *cis* and *HM* geometries. The steepness of this trend is sensitively reduced by using a B3LYP functional and without the Tamm–Dancoff approximation, but is still present and can have important effects on a simulation of the excited state dynamics of the isomerization process. This last consideration is also supported by a deep analysis on the potential energy surface of the Schiff bases performed by Wanko and collaborators in a previous work [50], and by previous TDDFT calculations [41] in which the atomic coordinates were calculated using ROKS. The discrepancies between TDDFT and other methods in the description of the MM isomerization are not a consequence of the different geometries used, since TDDFT, CASPT2 and MBPT S_1 energies are all calculated on the same CASSCF coordinates. Further help for the understanding of the MM isomerization process could come from an experimental evaluation of its velocity.

This work demonstrates that MBPT is an affordable and accurate technology for the evaluation of excited states energy surfaces of photoactive molecules.

Acknowledgement

We acknowledge support from EU e-I3 ETSF project no. 211956 (ETSF user projects no. 71 and no. 232). Computer resources granted by CINECA and ENEA CRESCO are gratefully acknowledged.

L.G. acknowledges the CASPUR computer centre for computational resources and the ERC project no. 240624. We thank Ari P. Seitsonen for critical reading of the manuscript.

References

- [1] G. Adragna, R. Del Sole, A. Marini, *Phys. Rev. B* 68 (16) (2003) 165108.
- [2] M. Arnaboldi, M.G. Motto, K. Tsujimoto, V. Balogh-Nair, K. Nakanishi, *J. Am. Chem. Soc.* 101 (23) (1979) 7082.
- [3] V. Balogh-Nair et al., *Photochem. Photobiol.* 33 (4) (1981) 483.
- [4] M.E. Casida, in: J.M. Seminario (Ed.), *Recent Developments and Applications of Modern Density Functional Theory*, Elsevier, Amsterdam, 1996.
- [5] A. Cembran, M. Olivucci, F. Bernardi, M. Garavelli, *PNAS* 102 (18) (2005) 6255.
- [6] A. Cembran, R. Gonzalez-Luque, P. Altoe, M. Merchan, F. Bernardi, M. Olivucci, M. Garavelli, *J. Phys. Chem. A* 109 (29) (2005) 6597.
- [7] R.F. Childs, G.S. Shaw, R.E. Wasylshen, *J. Am. Chem. Soc.* 109 (18) (1987) 5362.
- [8] S. Fantacci, A. Migani, M. Olivucci, *J. Phys. Chem. A* 108 (7) (2004) 1208.
- [9] N. Ferré, M. Olivucci, *J. Am. Chem. Soc.* 125 (2003) 6868.
- [10] A.L. Fetter, J.D. Walecka, *Quantum Theory of Many-Particle Systems*, McGraw-Hill, San Francisco, 1971.
- [11] L.M. Frutos, T. Andrúniów, F. Santoro, N. Ferré, M. Olivucci, *PNAS* 104 (19) (2007) 7764.
- [12] M. Garavelli, P. Celani, F. Bernardi, M.A. Robb, M. Olivucci, *J. Am. Chem. Soc.* 119 (29) (1997) 6891.
- [13] P.A. Hargrave et al., *Eur. Biophys. J.* 9 (4) (1983) 235.
- [14] L. Hedin, *Phys. Rev.* 139 (1965) A796.
- [15] R. Henderson, J.M. Baldwin, T.A. Ceska, F. Zemlin, E. Beckmann, K.H. Downing, *J. Mol. Biol.* 213 (4) (1990) 899.
- [16] E. Hendrickx, K. Clays, A. Persoons, C. Dehu, J.L. Bredas, *J. Am. Chem. Soc.* 117 (12) (1995) 3547.
- [17] H. Kandori, Y. Shichida, T. Yoshizawa, *Biochemistry (Moscow)* 66 (11) (2001) 1197.
- [18] T.W. Keal, M. Wanko, W. Thiel, *Theor. Chem. Acc.* 123 (1–2) (2009) 145.
- [19] T. Kobayashi, T. Saito, H. Ohtani, *Nature* 414 (2001) 531.
- [20] P. Kukura, D.W. McCamant, S. Yoon, D.B. Wandschneider, R.A. Mathies, *Science* 310 (2005) 1006.
- [21] Y. Ma, M. Rohlfing, C. Molteni, *Phys. Rev. B* 80 (2009) 241405.
- [22] Y. Ma, M. Rohlfing, C. Molteni, *J. Chem. Theory Comput.* 6 (1) (2010) 257.
- [23] M.S. Kaczmarek, Y. Ma, M. Rohlfing, *Phys. Rev. B* 81 (2010) 115433.
- [24] G.J. Martyna, M.E. Tuckerman, *J. Chem. Phys.* 110 (1999) 2810.
- [25] M. Merchan, R. Gonzalez-Luque, *J. Chem. Phys.* 106 (3) (1997) 1112.
- [26] C.K. Meyer, M. Böhme, A. Ockenfels, W. Gärtner, K.P. Hofmann, O.P. Ernst, *J. Bio. Chem.* 275 (26) (2000) 19713.
- [27] T.E. Meyer, E. Yakali, M.A. Cusanovich, G. Tollin, *Biochemistry* 26 (2) (1987) 418.
- [28] J. Nathans, D.S. Ogness, *PNAS* 81 (1984) 4851.
- [29] I.B. Nielsen, L. Lammich, L.H. Andersen, *Phys. Rev. Lett.* 96 (2006) 018304.
- [30] G. Onida, L. Reining, R.W. Godby, R. Del Sole, W. Andreoni, *Phys. Rev. Lett.* 75 (1995) 818.
- [31] G. Onida, L. Reining, A. Rubio, *Rev. Mod. Phys.* 74 (2) (2002) 601.
- [32] C.S. Page, M. Olivucci, *J. Comput. Chem.* 24 (3) (2003) 298.
- [33] A.B. Patel, E. Crocker, M. Eilers, A. Hirshfeld, M. Sheves, S.O. Smith, *PNAS* 101 (27) (2004) 10048.
- [34] J.P. Perdew, K. Burke, M. Ernzerhof, *Phys. Rev. Lett.* 77 (1996) 3865.
- [35] J.P. Perdew, A. Zunger, *Phys. Rev. B* 23 (10) (1981) 5048.
- [36] L. Reining, V. Olevano, A. Rubio, G. Onida, *Phys. Rev. Lett.* 88 (6) (2002) 066404.
- [37] U.F. Rohrig, L. Guidoni, A. Laio, I. Frank, U. Rothlisberger, *J. Am. Chem. Soc.* 126 (47) (2004) 15328.
- [38] U.F. Rohrig, L. Guidoni, U. Rothlisberger, *Biochemistry* 41 (35) (2002) 10799.
- [39] I.V. Rostov, R.D. Amos, R. Kobayashi, G. Scalmani, M.J. Frisch, *J. Phys. Chem. B* 114 (16) (2010) 5547.
- [40] E. Runge, E.K.U. Gross, *Phys. Rev. Lett.* 52 (12) (1984) 997.
- [41] F. Schautz, F. Buda, C. Filippi, *J. Chem. Phys.* 121 (12) (2004) 5836.
- [42] R. Send, D. Sundholm, *J. Phys. Chem. A* 111 (36) (2007) 8766.
- [43] R. Send, D. Sundholm, M.P. Johnsson, F. Pawłowski, *J. Chem. Theory Comput.* 5 (9) (2009) 2401.
- [44] F. Sottile, V. Olevano, L. Reining, *Phys. Rev. Lett.* 91 (5) (2003) 056402.
- [45] Z. Su, W. Liang, G. Chen, *Chem. Phys.* 247 (2) (1999) 185.
- [46] M. Sun, Y. Ding, G. Cui, Y. Liu, *J. Phys. Chem. A* 111 (15) (2007) 2946.
- [47] I. Tavernelli, U.F. Rohrig, U. Rothlisberger, *Mol. Phys.* 103 (2005) 963.
- [48] O. Valsson, C. Filippi, *J. Chem. Theory Comput.* 6 (4) (2010) 1275.
- [49] T. Vreven, F. Bernardi, M. Garavelli, M. Olivucci, M.A. Robb, H.B. Schlegel, *J. Am. Chem. Soc.* 119 (51) (1997) 12687.
- [50] M. Wanko, M. Garavelli, F. Bernardi, T.A. Niehaus, T. Frauenheim, M. Elstner, *J. Chem. Phys.* 120 (4) (2004) 1674.